Synthesis and structural investigation of an 'oxazinoquinolinespirohexadienone' that only exists as its long-wavelength ring-opened quinonimine isomer.

Benjamin J. Pollock,[a,b] Christos A. Sikes,[a,b] Ryan P. Ter Louw,[a] Scott R. Hawken,[a] Amy L. Speelman,[a] Eugene J. Lynch,[a] Daniel J. Stanford,[b] Kraig A. Wheeler,[c] Jason G. Gillmore[a]*

[a]Department of Chemistry, Hope College, 35 E. 12th St., Holland, MI 49423

[b]Department of Chemistry, Harper College, 1200 W. Algonquin Rd., Palatine, IL 60067

[c]Department of Chemistry, Eastern Illinois University, 600 Lincoln Ave., Charleston, IL 61920

Corresponding Author
*gillmore@hope.edu, 616.395.7308 (phone), 616.395.7118 (fax)

Author Contributions
The manuscript was written through contributions of all authors. All authors have given approval to the final version of the manuscript.

TOC Graphic / Graphical Abstract

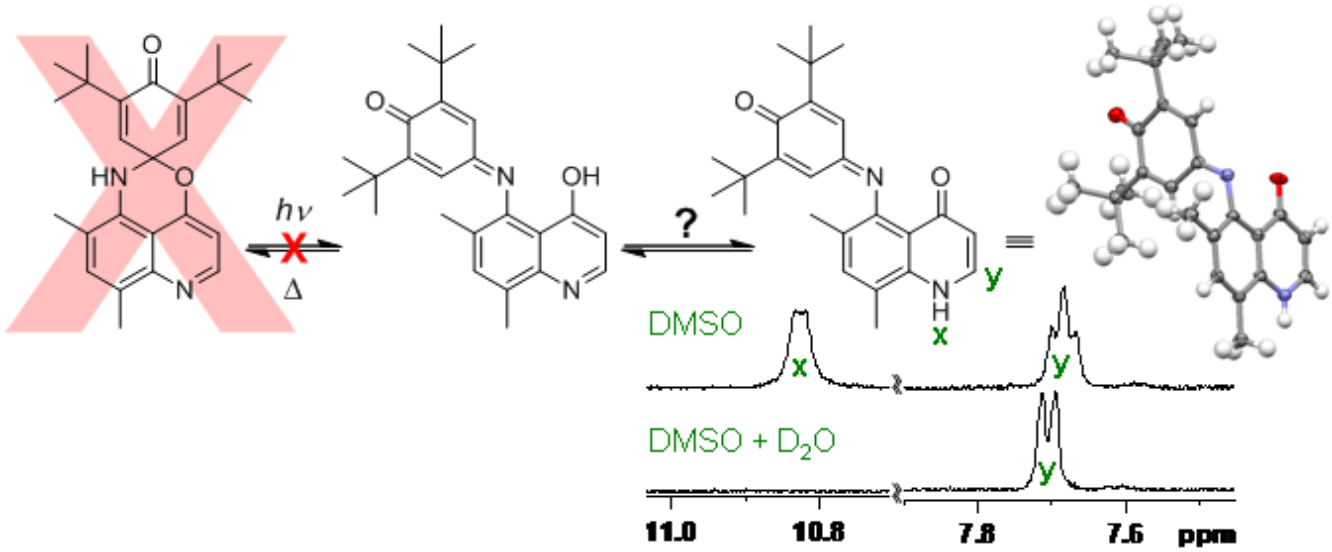

ABSTRACT

The spirocyclic oxazinoquinolinespirohexadienone (OSHD) "photochromes" are computationally predicted to be an attractive target as electron deficient analogs of the perimidinespirohexadienone (PSHD) photochromes, for eventual application as photochromic photooxidants. We have found the literature method for their preparation unsuitable, and present an alternative synthesis. Unfortunately the product of this synthesis is the long wavelength (LW) ring-opened quinonimine isomer of the OSHD. We have found this isomer does not close to the spirocyclic short wavelength isomer (SW) upon prolonged standing in the dark on, unlike other PSHD photochromes. The structure of this long wavelength isomer was found by NMR and X-ray crystallography to be exclusively the quinolinone (keto) tautomer, though experimental cyclic voltammetry supported by our computational methodology indicates that the quinolinol (enol) tautomer (not detected by other means) may be accessible through a fast equilibrium lying far towards the keto tautomer. Computations also support the relative stability order of keto LW over enol LW over SW.

Introduction

Our group focuses on designing and employing photochromes of the perimidinespirohexadienone (PSHD) family as possible "switchable" photooxidants. The PSHD family of photochromes offers many properties suitable for gating photoinduced charge transfer (PICT) reactions via photochromic rearrangements as discussed in detail in an earlier manuscript.[1] That manuscript focused on preparing analogs of the PSHDs in which the naphthalene moiety is replaced with a quinoline, resulting in the quinazolinespirohexadienones (QSHDs). These QSHDs are predicted to be more reducible than the parent PSHDs based on a computational method of predicting the ground-state reduction potentials of organic compounds we have reported[2],[3] which we have also confirmed experimentally.[4] Other promising analogs include the oxazinoquinolinespirohexadienones (OSHDs), where one of the bridging nitrogen atoms in the QSHDs is replaced with an oxygen atom. This oxygen, being a stronger inductive withdrawer and a weaker resonance donor than nitrogen, is predicted to make both the spirocyclic short-wavelength isomer (SW) and the open quinonimine long-wavelength isomer (LW) of the OSHDs even more reducible than the corresponding isomers of the QSHDs; this prediction is supported computationally (*vide infra*).

The literature available on these compounds reports photochromic, thermochromic, and solvatochromic behavior.[5] A synthetic procedure is also reported in which 4-chloro-2,8-dimethylquinolin-5-amine **3a** is coupled with 2,6-di-*tert*-butyl-1,4-benzoquinone (DBB) to yield the short-wavelength isomer (SW) of the corresponding OSHD **1a**; the synthesis of precursor **3a** is not reported, nor is this compound commercially available. Our attempts to couple a very similar compound (differing only in methyl substitution) with DBB by this procedure yielded a different product. We herein report an alternative synthesis of the OSHD LW **2b**, which ultimately proved to exist solely as its long-wavelength quinonimine isomer (LW) expressing no characteristic photochromic behavior.

Results and Discussion

Scheme 1.

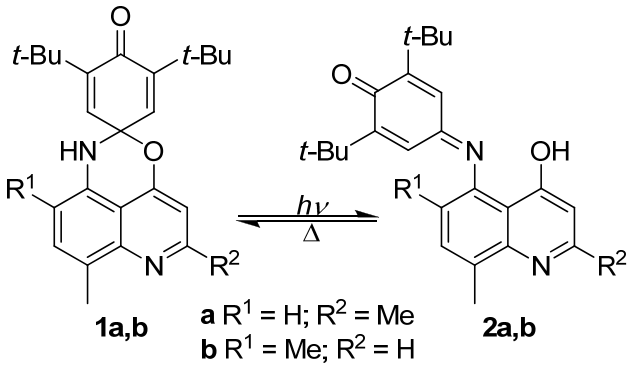

The synthesis of **1a** reported in the literature was not attempted as the preparation of precursor **3a** is not reported.[5] Instead, working from **3b**, an intermediate we reported in our previous QSHD work,[1] we attempted the identical procedure to couple with 2,6-di-*tert*-butyl-1,4-benzoquinone (DBB) without success. The anticipated formation of **1b** was not observed. Instead, the reaction yielded **4**, in which the displacement of the chlorine atom did not occur (Scheme 2), and we were unable to hydrolyze **4** to **1b/2b**.

Scheme 2.

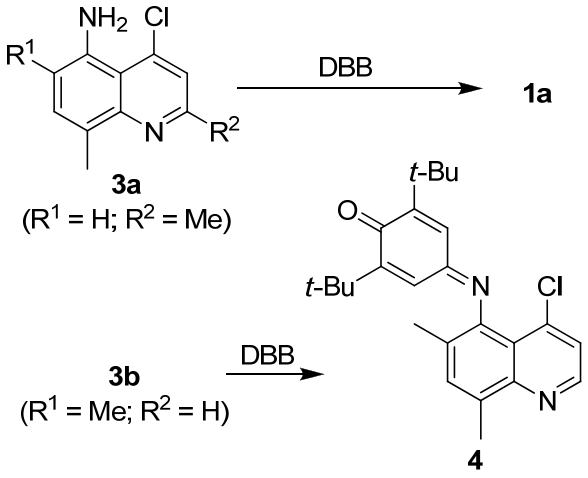

These unsuccessful attempts at making **1b/2b** forced us to consider a new synthetic route (Scheme 3). This new course of reactions was begun from another readily available intermediate **5** also reported in our QSHD synthesis,[1] and was designed to allow DBB to serve solely as an electrophile, rather than as both nucleophile and electrophile. First, electrophilic nitration of **5** yielded **6**. Palladium-catalyzed hydrogenation followed to reduce the nitro group of **6** to its nucleophilic amino counterpart resulting in the formation of **7**. Coupling with DBB to form the colored, LW isomer **2b** was successful; however, the presence of this quinonimine LW isomer at dark equilibrium indicated the lack of its ability to undergo thermal bleaching to the desired SW isomer, **1b**. This dilemma was further aggravated by the pair of tautomers possible for the LW isomer, **2b** and **2'b** (as well as for intermediates **5-7**).

Scheme 3.

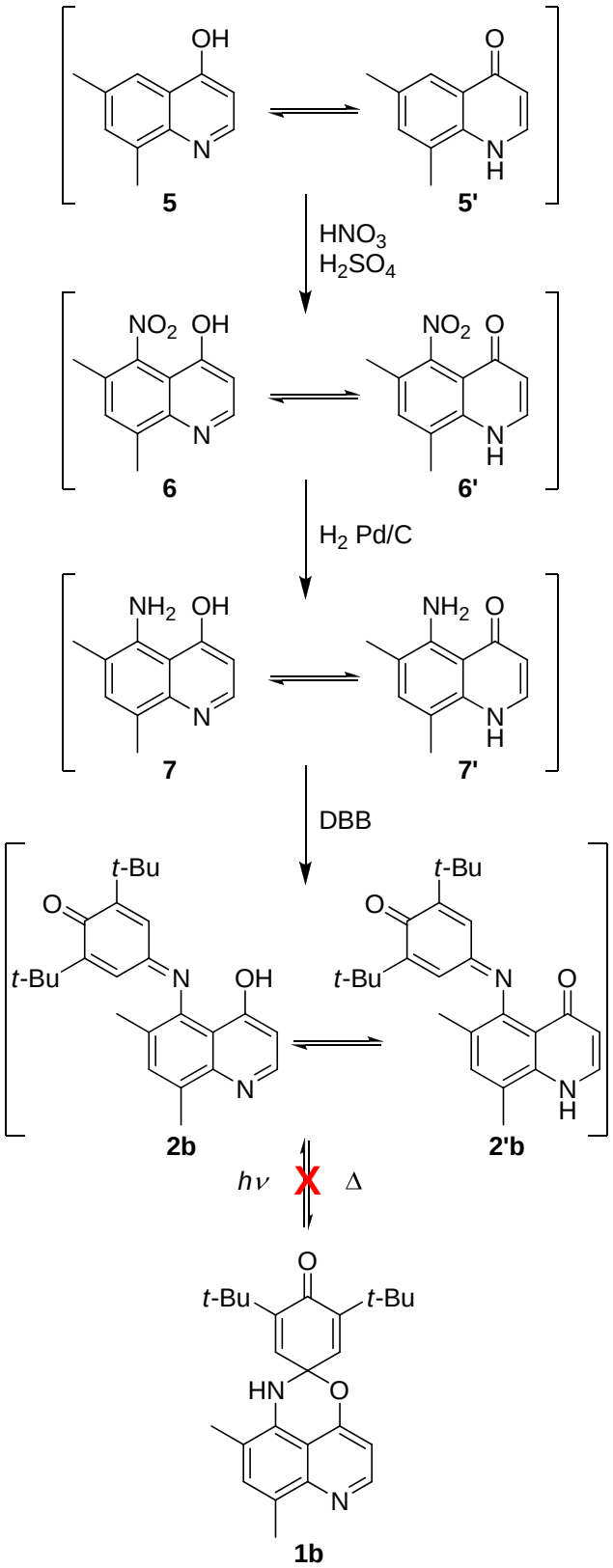

The lack of photochromism observed between **2b/2'b** and **1b** was initially hypothesized to have been the result of nitration occurring in a location other than the C5 position of quinoline **5/5'**. This possibility was tested by hydrolyzing **8** and **3b** (both intermediates from our QSHD synthesis) under acidic conditions. These hydrolyses conclusively yielded **6/6'** and **7/7'**, respectively, thus confirming the desired regioselectivity of the nitration reaction. Inspired by this success, we attempted the analogous hydrolysis of **4** in an attempt to form **2b/2'b**, but all conditions that were able to hydrolyze the chlorine atom also hydrolyzed the imine thus decomposing **4** to give **7/7'**.

Scheme 4.

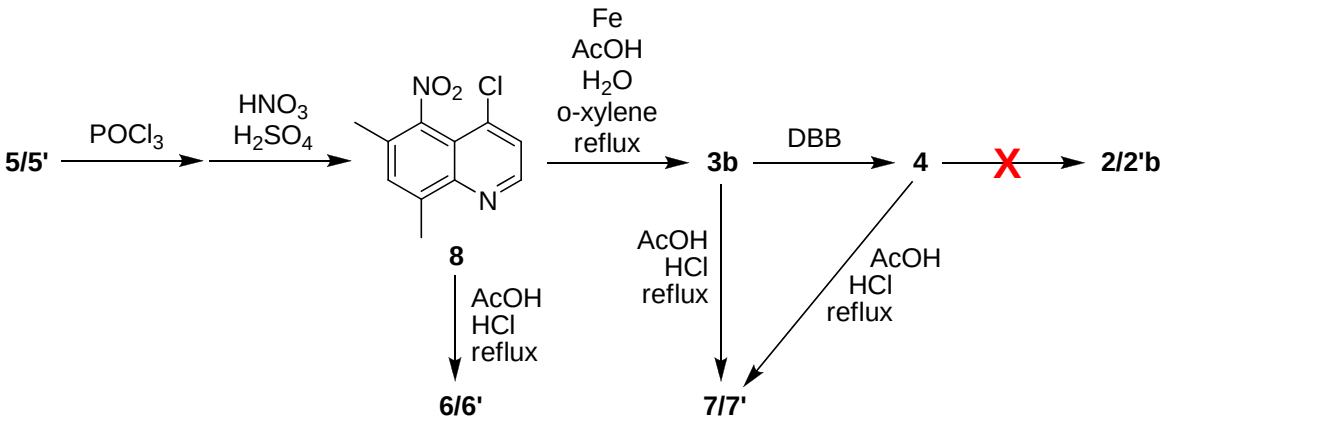

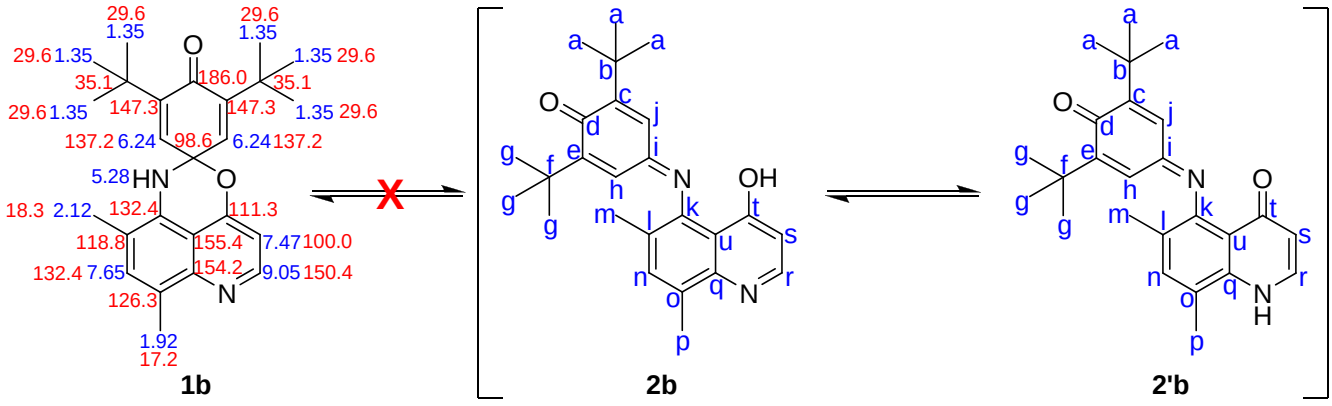

Figure 1. NMR chemical shifts and atom labeling.

Structural investigation of the isolated **2b/2'b** to determine in which tautomer this compound exists was begun with NMR analysis. Comparisons of experimental ^{1}H and ^{13}C chemical shifts with those predicted by *ChemDraw's ChemNMR* predictor were made. Predictions of the chemical shifts for **1b** are labeled on the structure in Figure 1—^{1}H shifts in blue and ^{13}C shifts in red—while atom labels on **2b/2'b** correspond to the lettering used in Tables 1 and 2. Note that the predicted values do not reflect spatial differences between atoms in otherwise equivalent chemical environments. ^{13}C NMR experimental chemical shifts do not conclusively point to one tautomer or the other with respect to predicted values, however, the experimentally observed chemical shifts of 187.2 ppm and 177.3 ppm are consistent with the presence of two carbonyl groups (i.e., **2'b)**. Upfield experimental ^{1}H NMR chemical shifts agree well with predictions for both tautomers; however, in the aromatic region of the spectrum experimental results reflect values slightly closer to the chemical shifts predicted for **2'b**, though these results would alone be far from conclusive. Additionally, the presence of a ^{1}H NMR signal at 10.83 ppm would be more anomalous for the phenolic proton in structure **2b** predicted at 5.35 ppm, than for the vinylagous amide proton of **2'b** for which *ChemNMR* was unable to provide an accurate prediction.

Table 1. ^{13}C NMR predicted and experimental chemical shifts.

Carbon[a]	Predicted (ppm) for **2b**	Predicted (ppm) for **2'b**	Experimental (ppm)
a	29.3	29.3	29.0
b	34.9	34.9	34.8
c	148.9	148.9	151.2
d	186.0	186.0	187.2
e	148.9	148.9	151.4
f	34.9	34.9	34.9
g	29.3	29.3	29.2
h	141.8	141.8	138.1
i	164.6	164.6	156.3
j	141.8	141.8	138.3
k	138.4	141.6	145.0
l	130.0	120.9	117.8
m	19.0	18.6	17.3
n	133.6	138.8	134.2
o	134.4	127.9	121.0
p	17.2	18.0	17.0
q	155.1	143.3	134.4
r	150.8	139.5	121.6
s	108.7	108.8	110.2
t	165.9	182.1	177.3
u	111.9	116.6	116.1

[a]As labeled in Figure 1.

Table 2. ^{1}H NMR predicted and experimental chemical shifts.

Proton[a]	Predicted for **2b**	Predicted for **2'b**	Experimental (ppm)
a	1.35	1.35	1.03
g	1.35	1.35	1.32
h	6.47	6.47	6.33
j	6.47	6.47	7.11
m	2.34	2.34	2.42
n	7.81	7.13	7.38
p	1.92	2.12	1.88
r	9.01	6.98	7.68
s	7.48	7.15	5.85
X-H[b]	5.35	4.00	10.83

[a]As labeled in Figure 1. [b]X = O (**2b**), N (**2'b**)

In conjunction with the previous NMR results, a deuterium exchange experiment was carried out on the product sample to verify that the X-H proton was responsible for the signal at 10.83 ppm; the addition of D_2O was indeed followed by the fading of this signal. Although this result alone does not indicate the presence of one tautomer over the other, the concurrent change in multiplicity of the signal at 7.68 ppm from a triplet to a doublet (Figure 2) is very telling. This change in multiplicity clearly indicates that the X-H proton, itself appearing as a fine doublet in our best resolved spectra, interacts with the adjacent proton r—consistent only with the constitution of the LW isomer as the quinolinone keto tautomer **2'b**.

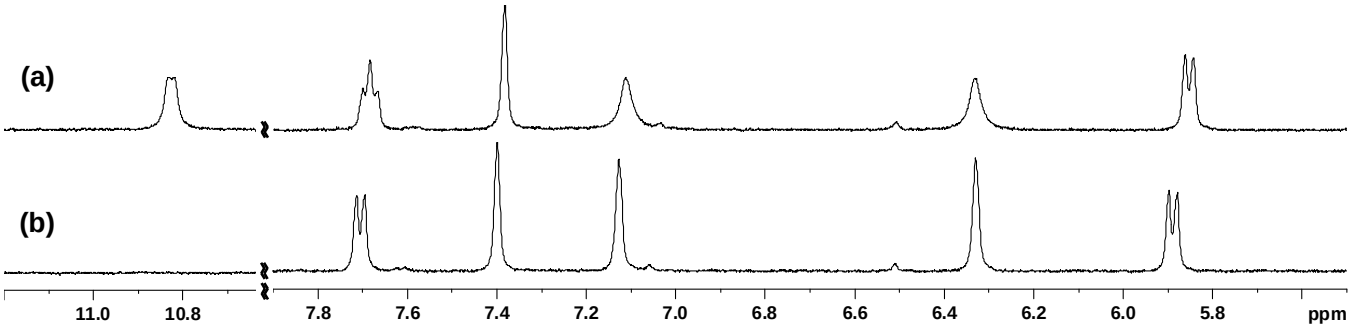

Figure 2. Deuterium exchange experiment: (a) ^{1}H NMR of **2'b** in DMSO-d6, (b) the same sample upon addition of 1 drop of D_2O.

To confirm the solution NMR results, crystals were grown for an X-ray diffraction study to confirm the solid-state structural identity of **2b/2'b**. The diffraction pattern was solved to definitively identify the structure as quinolinone keto tautomer **2'b**. It was possible to actually locate and refine the position of the hydrogen atom on the quinoline nitrogen atom (and the lack thereof on the oxygen atom) from an electron density map. Furthermore, bond lengths that are consistent with the quinolinone (keto) structure are observed. Together these x-ray data provide very strong evidence that the obtained LW isomer exists solely as **2'b** in the solid state, as well as in solution.

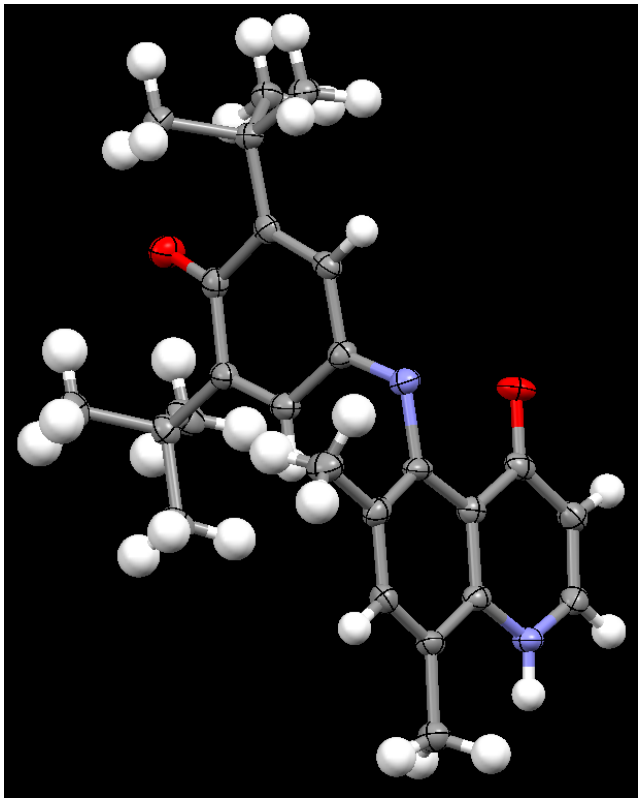

Figure 3. Crystal structure of **2'b** displayed with thermal ellipsoids at 50% probability.

Due to a similar pair of tautomers possible in synthetic intermediates **5/5'**-**7/7'**, analogous NMR experiments were carried out on these compounds. In each case, the presence of a ^{13}C NMR signal appearing at $\geq$173.95 ppm is consistent with the presence of the carbonyl carbons required by keto structures **5'**, **6'**, and **7'**. Furthermore, deuterium exchange experiments with D_2O that were carried out on these intermediates produced exactly analogous results as that for **2'b**; that is, both the disappearance of the furthest downfield signal and the change in multiplicity of the signal for the proton adjacent to the quinoline nitrogen from a triplet to a doublet. In addition to NMR experiments, crystals were grown of **5/5'** for an X-ray diffraction study. The results obtained from this investigation revealed the same constitutional pattern as **2'b** in both the presence of a hydrogen atom on the quinoline nitrogen and bond

lengths consistent with the quinolinone tautomer **5'**. Crystals suitable for X-ray diffraction were unable to be grown from **6/6'** and **7/7'** due to solubility issues.

Table 3. B3LYP energies and tautomer equilibria.

Cmpd	Energy of Quinolinol, **X** (E_h)	Energy of Quinolinone, **X'** (E_h)	ΔE (E_h)	ΔE (kcal/mol)	Calculated K	Calculated Percent Quinolinone, **X'**
2a/2'a	-1231.03019	-1231.03178	-0.00160	-1.00	5.42	84.4
2b/2'b	-1231.02281	-1231.02543	-0.00262	-1.64	16.1	94.1
5/5'	-555.95590	-555.96482	-0.00892	-5.60	1.26×10^4	99.9921
6/6'	-760.51040	-760.51967	-0.00928	-5.82	1.85×10^4	99.9946
7/7'	-611.33087	-611.34581	-0.01494	-9.37	7.45×10^6	99.99999

Finally, the experimental results regarding the tautomers observed were confirmed computationally. Energies of both pairs of tautomers of compounds **5**-**7** and **2b** were calculated at B3LYP/6-311+G(d,p) with implicit acetonitrile by CPCM[6,7] on geometries optimized in the gas-phase at B3LYP/6-31G(d) or MIDI!. The difference in computed energy between tautomers of a given species, ΔE, provided a means of estimating the equilibrium constants and corresponding Boltzmann distributions of the respective tautomers (Table 3). In each case, the energy calculated for the quinolinone tautomer reflects a greater stability than that of the quinolinol tautomer; the literature[5] fails to mention the presence of the apparently more stable tautomer **2'a** over **2a** while in our case the presence of **2'b** dominates that of **2b** in addition to all similar synthetic intermediates. Furthermore, the energy computed for SW isomer **1b** (-1231.00869 E_h) is less negative than that of either LW tautomer, **2b** or **2'b**, explaining why the LW isomer is exclusively present even after prolonged standing in the dark in the solid state or in solution. Similar results were obtained for **1a** (-1231.01820 E_h) being less

stable than either **2a** or **2'a**, and **2'a** being favored over **2a**. Admittedly the difference between these two LW tautomers for Postupnaya's regioisomer[5] is less than for ours.

Finally, we sought to employ cyclic voltammetry to confirm the solution structure of **2'b** and simultaneously validate our computational method for predicting ground-state reduction potentials, which we have demonstrated to be accurate to within about 100 mV for a wide range of structures, including very close analogs of these photochromes.[3] Interestingly, the observed voltammogram of a solution of **2'b** yielded an experimental reduction potential of -0.67 V vs SCE, which is consistent with the reduction potential our method would predict for quinolinol tautomer **2b** (-0.72 V vs SCE) rather than for **2'b** (-1.13 V vs SCE). This reduction potential was observed regardless of scan rate (from 10 – 10,000 mV/sec), and indicates that **2'b** must be in rapid equilibrium with **2b** in solution, even though **2b** is not present in quantities detectable by NMR (regardless of solvent or the presence or absence of electrolyte in solution.)

Conclusion

The literature route reported for preparing **1a**[5] failed to yield **1b** in our hands. We devised a more straightforward route to the OSHD photochromes, only to find that we failed to isolate the SW isomer **1b**, but rather a quinonimine LW isomer. This LW has been conclusively demonstrated to exist as the quinolinone (keto) tautomer **2'b**, both in solution and in the crystalline solid state. This appears reasonable on the basis of computations that demonstrate the greater thermodynamic stability of **2'** over both its quinolinol (enol) tautomer **2** and the spirocyclic SW isomer **1** for our regioisomer, and to a lesser extent, Postupnaya's as well. Cyclic voltammetry, in concert with our computational method for predicting ground-state reduction potentials,[3] does provide evidence of a rapid equilibrium between **2'b** and **2b** (even though our other data indicate this equilibrium lies far toward the keto tautomer.)

Furthermore, this application serves as a validation of our computational method and suggests it will be useful in designing future photochromic photooxidant targets.

Experimental

General Methods. ^{1}H and ^{13}C NMR spectra were recorded on 400 MHz instruments. Chemical shifts are given in ppm relative to appropriate solvent residual signals ($CDCl_3$, DMSO-d6) reported in the literature.[8] NMR experiments involving proton/deuterium exchange were done by adding 1-2 drops of D_2O to existing NMR samples and shaking vigorously before recording the deuterium-exchanged spectra.

All calculations were performed on the MU3C cluster[9] at Hope College implemented through the *WebMO*[10] graphical user interface using density functional theory (DFT) on *Gaussian03*[11] with the Becke 3 Lee, Yang, and Parr (B3LYP) hybrid functional. Single-point energies were calculated with implicit acetonitrile solvent by the conductor-like polarizable continuum model (CPCM) using the default UA0 radii at 6-311+G(d,p) on gas-phase geometries computed at B3LYP/MIDI! or 6-31G(d). Computationally predicted reduction potentials were obtained using correlation 7 from our recently published manuscript.[3]

Cyclic voltammetry was conducted using a glassy carbon working electrode, platinum wire counter electrode, and a non-aqueous $Ag/AgNO_3$ reference electrode. Reference (10 mM $AgNO_3$) and analyte solutions (1 mM) were freshly prepared in solutions of dry acetonitrile (similar results also obtained in dry DMSO) containing 0.1 M tetrabutylammonium hexafluorophosphate as supporting electrolyte, and experiments were conducted on argon-deaerated solutions under a gently flowing dry argon blanket. Results were normalized to ferrocene/ferrocenium by back-to-back experiments (which also served to set iR compensation), and were then corrected to vs SCE.[12,13]

GC/MS characterization was performed through a 30 m × 0.25 mm × 0.25 μm Agilent HP-5ms or equivalent capillary column at a flow rate of 0.93 mL/min of UHP He carrier gas. One-μL samples of solutions of approximately 0.2 mg/mL concentration were injected into the split/splitless injector at 250 °C at a 50:1 split ratio. The initial oven temperature of 50 °C was held for 5 minutes then ramped to 200 °C at 10 °C/min, then to 320 °C at 20 °C/min then held there for 10 minutes. The transfer line temperature was 280 °C into a 70 eV electron impact source at 230 °C with a quadrupole temperature of 150 °C. HRMS data was obtained by direct probe with electron impact ionization.

Crystals of **2'b** were grown from THF/pentane via a vapor-diffusion method.[14] For synthetic intermediate **5'**, crystals were grown from 1-propanol/pentane using a liquid-layering technique referred to as solvent diffusion.[14] X-ray data were collected at 100 K on a CCD diffractometer equipped with a graphite-monochromator using Cu Kα radiation (λ=1.54178 Å). Data sets were corrected for Lorentz and polarization effects as well as absorption. The criterion for observed reflections is $I > 2\sigma(I)$. Lattice parameters were determined from least-squares analysis and reflection data. Empirical absorption corrections were applied using *SADABS*.[15] The structures were solved by direct methods and refined by full-matrix least-squares analysis on F^2 using *X-SEED*[16] equipped with *SHELXS*[17]. All non-hydrogen atoms were refined anisotropically by full-matrix least-squares on F^2 by the use of the *SHELXL*[17] program. NH hydrogens in **2'b** and **5'** were located in difference Fourier synthesis and refined with U_{iso}=1.2U_{eq} and N-H distances restrained to 0.85(2) Å. The remaining H atoms were included in idealized geometric positions with U_{iso}=1.2U_{eq} of the atom to which they were attached (U_{iso}=1.5U_{eq} for methyl groups).

Compounds **3b**, **5'**, and **8** were prepared as previously reported.[1] All other compounds were purchased commercially in the highest purity available and used as received, except for acetonitrile, DMF, and DMSO, which were dispensed from a column-based dry solvent purification system.

2,6-di-*tert*-butyl-4-(4-chloro-6,8-dimethylquinolin-5-ylimino)cyclohexa-2,5-dienone (4). In an adaptation of a literature procedure,[5] in an attempt to prepare **1b**, a mixture of 2,6-di-*tert*-butyl-1,4-benzoquinone (DBB, 0.107 g, 0.49 mmol), **3b** (0.101 g, 0.49 mmol), and anhydrous TsOH (0.0042 g, 0.024 mmol, prepared by heating TsOH•H_2O in an argon-purged, evacuated flask on a 100 °C oil bath until solid melted and water evolution ceased) was stirred at 150 °C in an oil bath for 18 h under argon. After cooling to room temperature, purification of the resultant dark solid by preparative thin layer chromatography on silica gel (20:80 EtOAc/hexane) yielded 0.0224 g (11%) of a dark red solid (**4**). mp 145-147 °C; ^{1}H NMR (400 MHz, DMSO-d_6): δ (ppm) 8.76 (d, 1H), 7.67 (s, 1H), 7.61 (d, 1H), 7.19 (d, 1H), 6.26 (d, 1H), 2.69 (s, 3H), 2.02 (s, 3H), 1.32 (s, 9H), 1.02 (s, 9H); ^{13}C NMR (400 MHz, $CDCl_3$): δ (ppm) 187.6, 160.2, 154.1, 154.0, 148.4, 148.0, 142.2, 141.1, 134.1, 133.6, 133.5, 123.4, 122.5, 121.6, 119.2, 35.66, 35.64, 29.7, 29.5, 19.0, 18.8; GC/MS rt 26.019 min. (*m/z* 408/410, 351); HRMS (EI) *m/z*: calcd for $C_{25}H_{29}ClN_2O$ 408.1968, found 408.1972.

6,8-dimethylquinolin-4(1*H*)-one (5'). Prepared as previously reported.[1] mp 223-228 °C; ^{1}H NMR (400 MHz, DMSO-d_6): δ (ppm) 11.04 (br s, 1H), 7.78 (t, 1H), 7.75 (s, 1H), 7.33 (s, 1H), 6.02 (d, 1H), 2.44 (s, 3H), 2.36 (s, 3H); ^{13}C NMR (400 MHz, DMSO-d_6): δ (ppm) 176.9, 139.0, 137.8, 133.8, 131.8, 126.2, 125.8, 122.1, 108.4, 20.6, 17.1; GC/MS rt 23.176 min. (*m/z* 173, 158, 144, 130).

6,8-dimethyl-5-nitroquinolin-4(1*H*)-one (6'). In an adaptation to the literature method,[1] a flask containing concentrated H_2SO_4 (17 mL) was slowly charged with **5'** (7.5215 g, 43.42 mmol) at 0 °C, creating a dark brown solution. A mixture of concentrated H_2SO_4 (3.4 mL) and fuming (90%) HNO_3 (4.1 mL) was added drop-wise to the solution while stirring at 0 °C. The reaction mixture was stirred at 0 °C for 1 h and then added to a 2-L flask containing 300 g of ice. Once the ice had melted, the light tan mixture was slowly neutralized with saturated aqueous sodium carbonate (220 mL). Vacuum filtration of the mixture through a medium-porosity frit yielded a clay-like tan solid. Vacuum drying yielded

8.9457 g (94.4%) of a light tan solid (**6'**). mp 300-330 °C (dec); ^{1}H NMR (400 MHz, DMSO-d_6): δ (ppm) 11.42 (br s, 1H), 7.88 (t, 1H), 7.56 (s, 1H), 6.09 (d, 1H), 2.49 (s, 3H), 2.20 (s, 3H); ^{13}C NMR (400 MHz, DMSO-d_6): δ (ppm) 174.0, 145.5, 139.6, 137.6, 134.4, 129.0, 123.3, 116.1, 109.9, 17.2, 15.3; GC/MS rt 25.276 min. (*m/z* 218, 188, 171, 143, 115). HRMS (EI) *m/z*: calcd for $C_{11}H_{10}N_2O_3$ 218.0691, found 218.0696.

*Hydrolysis of **8** to prove structure of **6'**.* A round-bottom flask fitted with a water-cooled condenser was charged with **8** (0.0505 g, 0.21 mmol) with acetic acid (1 mL) and HCl (0.5 mL). The clear, yellow mixture was stirred in a 115 °C oil bath for 22 h. Upon cooling to room temperature, a yellowish solid precipitated. The mixture was added to water (~20 mL) and neutralized with 2M NaOH. Vacuum filtration afforded 0.0278 g (60%) of a pale yellow solid (**6'**). mp 300-330 °C (dec); ^{1}H NMR (400 MHz, DMSO-d_6): δ (ppm) 11.42 (br s, 1H), 7.88 (d, 1H), 7.56 (s, 1H), 6.09 (d, 1H), 2.49 (s, 3H), 2.20 (s, 3H); GC/MS rt 25.207 min. (*m/z* 218, 188, 171, 143, 115).

5-amino-6,8-dimethylquinolin-4(1*H*)-one (7'). A solution was prepared by dissolving **6'** (4.5108 g, 20.67 mmol) in DMF (400 mL); gentle heating was required to effect dissolution. The resulting orange solution was added to a 500-mL heavy-walled bottle, along with 0.45 g of 10% palladium on carbon (0.42 mmol Pd). The bottle was placed in a Parr hydrogenator, deaerated by repeated purging with nitrogen, then charged with hydrogen to a pressure of 60 psi and shaken, with hydrogen pressure in the 100 mL headspace maintained above 50 psi until three equivalents of H_2 had been absorbed and hydrogen uptake ceased. The apparatus was again purged with nitrogen before opening to atmosphere, at which point the black mixture was filtered through celite. Rotary evaporation of the dark orange filtrate followed by vacuum drying yielded 3.668 g (94.3%) of a dark brown solid (**7'**). mp 214-217 °C; ^{1}H NMR (400 MHz, DMSO-d_6): δ (ppm) 10.55 (br d, 1H), 7.59 (t, 1H), 7.23 (br s, 2H), 7.04 (s, 1H), 5.86 (d, 1H), 2.22 (s, 3H), 2.02 (s, 3H); ^{13}C NMR (400MHz, DMSO-d_6): δ (ppm) 181.7, 146.5, 138.4,

137.9, 135.1, 112.4, 111.9, 108.7, 108.6, 16.7, 16.5; GC/MS rt 24.291 min. (*m/z* 188, 187, 173). HRMS (EI) *m/z*: calcd for $C_{11}H_{12}N_2O$ 188.0950, found 188.0948.

*Hydrolysis of **3b** to prove structure of **7'***. A round-bottom flask was charged with **3b** (0.10660 g, 0.52 mmol) with acetic acid (2 mL) and HCl (1 mL) and equipped with a water-cooled condenser. The clear, red mixture was stirred and refluxed for 22 h. Upon cooling to room temperature, a solid precipitated from solution. The mixture was added to ~20 mL water and neutralized with 2M NaOH, then stirred on an ice bath for 5 minutes. Vacuum filtration allowed the isolation of 0.0615 g (63%) of a brown solid (**7'**). mp 218-222 °C; ^{1}H NMR (400 MHz, DMSO-d_6): δ (ppm) 10.55 (br d, 1H), 7.59 (t, 1H), 7.21 (br s, 2H), 7.03 (s, 1H), 5.86 (d, 1H), 2.22 (s, 3H), 2.02 (s, 3H); GC/MS rt 24.291 (*m/z* 188, 187, 173).

5-(3,5-di-*tert*-butyl-4-oxocyclohexa-2,5-dienylideneamino)-6,8-dimethylquinolin-4(1*H*)-one (2'b). A round-bottom flask was charged with **7'** (1.2155 g, 6.46 mmol) and DBB (1.5668 g, 7.112 mmol). A magnetic stir-bar and 1-propanol (17.6 mL) were added and a water-cooled condenser was attached. The reaction was brought to reflux and held there for 50-120 h, monitoring by TLC. After cooling to room temperature, volatiles were removed by rotary evaporation to yield yielding 2.3840 g of a dark black residue (94% crude yield). The solid residues of several reaction runs were combined. A total of 3.5715 g crude product was purified by column chromatography through 230-400 mesh silica gel, eluting with90:5:5 $CHCl_3$/DMF/triethylamine. This yielded 0.2407 g (6.7% recovery)of a dark red solid after vacuum drying. mp 170-190 °C (dec); ^{1}H NMR (400 MHz, DMSO-d_6): δ (ppm) 10.83 (fine d, 1H), 7.68 (t, 1H), 7.38 (s, 1H), 7.11 (s, 1H), 6.33 (s, 1H), 5.85 (d, 1H), 2.42 (s, 3H), 1.88 (s, 3H), 1.32 (s, 9H), 1.03 (s, 9H); ^{13}C NMR (400 MHz, DMSO-d_6): δ (ppm) 187.2, 177.3, 156.3, 151.4, 151.2, 145.0, 138.3, 138.1, 134.4, 134.2, 121.6, 121.0, 117.8, 116.1, 110.2, 34.9, 34.8, 29.2, 29.0, 17.3, 17.0; GC/MS rt 26.689 min. (*m/z* 390, 375, 187).

*Attempted hydrolysis of **4** to **2'b** (obtaining **7'**).* A round-bottom flask was charged with **4** (0.0504 g, 0.12 mmol) with acetic acid (1 mL) and HCl (0.5 mL). The clear, red mixture was stirred at reflux for 24 h under argon. The resultant black mixture was added to ~20 mL of water and neutralized with 2 M NaOH. After the mixture was neutralized, it was vacuum filtered through a medium-porosity frit to isolate 0.026 g (54%) of a black solid. Characterization revealed that both the chlorine atom and the imine had been hydrolyzed, resulting in **7'**. ^{1}H NMR (400 MHz, DMSO-d_6): δ (ppm) 10.56 (br s, 1H), 7.59 (t, 1H), 7.17 (br s, 2H), 7.03 (s, 1H), 5.86 (d, 1H), 2.21 (s, 3H), 2.02 (s, 3H); GC/MS rt 24.164 (*m/z* 188, 187, 173).

ACKNOWLEDGMENT

Work at Hope College was funded primarily by an NSF CAREER award to JGG (CHE-0952768), with initial work supported by a Camille & Henry Dreyfus Foundation Start-up Award (SU-04-440), a Research Corporation Cottrell College Science Award (CC6653) and start-up funding from the Hope College Department of Chemistry and Division of Natural & Applied Science. Support for work done at Harper College by DJS, BJP, and CAS was provided by the NSF STEM-ENGINES URC (CHE-0629174). EJL (home institution College of the Canyons, Santa Clarita, CA) was supported by an NSF REU SITE award (CHE-0851194) to Hope College. Computations were conducted on the Midwest Undergraduate Computational Chemistry Consortium (MU3C) cluster, supported by NSF MRI grants CHE-0520704 and CHE-1039925, housed in the Hope College Computational Science & Modeling Laboratory. Support from CSM Laboratory staff member Mr. Paul VanAllsburg and current and former directors Profs. Brent Krueger and Will Polik are acknowledged with gratitude. X-Ray diffraction conducted at Eastern Illinois University was performed on instrumentation funded by an NSF MRI grant (CHE- 0722547) by KAW. HRMS performed by Dr. Mike Walla at the University of South Carolina at short notice is gratefully acknowledged, as is additional support regarding HRMS from Dean Moses Lee (Hope College) and Dr. K. C. Harich (Virginia Tech).

Supporting Information. Complete spectral data (^{1}H & ^{13}C NMR, GC/MS, and diamond anvil ATR IR) for compounds **2'b**, **4**, **5'**, **6'**, and **7'** (including deuterium exchange NMR experiments for **2'b**, **5'**, **6'**, and **7'**, additional ^{1}H NMR and GC/MS data for compounds **6'** and **7'** formed by hydrolyses of **8** and **3b** and **4**, respectively, and 50% thermal ellipsoid image of **5'**), X-ray crystallography CIF files for **2'b** and **5'**, and computational data for **1a,b**, **2a,b**, **2'a,b**, **5**, **5'**, **6**, **6'**, **7**, and **7'**. This material is available free of charge via the Internet at http://pubs.acs.org.

REFERENCES

[1] Moerdyk, J.P., et al. *J. Photochem. Photobiol. A*, **2009**, *205*, 84.

[2] Speelman, A.L. and Gillmore, J.G. *J. Phys. Chem. A* **2008**, *112*, 5684.

[3] Lynch, E. J.; Speelman, A. L.; Curry, B. A.; Murillo, C. S.; Gillmore, J. G. *J. Org. Chem.* **2012**, *77*, 6423.

[4] Sluiter, K.B.; Moerdyk, J.P.; Speelman, A.L.; Lynch, E.J.; Gillmore, J.G. manuscript in preparation.

[5] Postupnaya, E.N.; Komissarov, V.N.; Kharlanov, V.A. *Zh. Org. Khim.*, **1993**, *29*, 1915.

[6] Barone, V.; Cossi, M. *J. Phys. Chem. A* **1998**, *102*, 1995.

[7] Cossi, M.; Rega, N.; Scalmani, G.; Barone, V. *J. Comput. Chem.* **2003**, *24*, 669.

[8] Fulmer, G.R.; Miller, A.J.M.; Sherden, N.H.; Gottlieb, H.E.; Nudelman, A.; Stoltz, B.M.; Bercaw, J.E.; Goldberg, K.I. *Organometallics* **2010**, *29*, 2176-79.

[9] Kuwata, K.T.; Kohen, D.; Krueger, B.P.; Polik, W.F. *Counc. Undergrad. Res. Q.* **2012**, *32* (4), 9.

[10] Schmidt, J.R.; Polik, W.F. *WebMO Pro*, v. 9.1; *WebMO Enterprise*, v. 10.1; WebMO LLC: Holland, MI, USA, 2009, 2010; available from http://www.webmo.net (accessed July 25, 2012).

[11] Frisch, M. J.; Trucks, G. W.; Schlegel, H. B.; Scuseria, G. E.; Robb, M. A.; Cheeseman, J. R.; Montgomery, Jr., J. A.; Vreven, T.; Kudin, K. N.; Burant, J. C.; Millam, J. M.; Iyengar, S. S.; Tomasi, J.; Barone, V.; Mennucci, B.; Cossi, M.; Scalmani, G.; Rega, N.; Petersson, G. A.; Nakatsuji, H.; Hada, M.; Ehara, M.; Toyota, K.; Fukuda, R.; Hasegawa, J.; Ishida, M.; Nakajima, T.; Honda, Y.; Kitao, O.; Nakai, H.; Klene, M.; Li, X.; Knox, J. E.; Hratchian, H. P.; Cross, J. B.; Bakken, V.; Adamo, C.; Jaramillo, J.; Gomperts, R.; Stratmann, R. E.; Yazyev, O.; Austin, A. J.; Cammi, R.; Pomelli, C.; Ochterski, J. W.; Ayala, P. Y.; Morokuma, K.; Voth, G. A.; Salvador, P.; Dannenberg, J. J.; Zakrzewski, V. G.; Dapprich, S.; Daniels, A. D.; Strain, M. C.; Farkas, O.; Malick, D. K.; Rabuck, A. D.; Raghavachari, K.; Foresman, J. B.; Ortiz, J. V.; Cui, Q.; Baboul, A. G.; Clifford, S.; Cioslowski, J.;

Stefanov, B. B.; Liu, G.; Liashenko, A.; Piskorz, P.; Komaromi, I.; Martin, R. L.; Fox, D. J.; Keith, T.; Al-Laham, M. A.; Peng, C. Y.; Nanayakkara, A.; Challacombe, M.; Gill, P. M. W.; Johnson, B.; Chen, W.; Wong, M. W.; Gonzalez, C.; Pople, J. A. Gaussian 03, Revision D.01, Gaussian, Inc.: Wallingford, CT, 2004.

[12] Bard, A. J.; Faulkner, L. R. *Electrochemical Methods: Fundamentals and Applications*, 2nd ed.; John Wiley & Sons: New York, 2000.

[13] Pavlishchuk, V. V.; Addison, A. W. *Inorg. Chim. Acta* **2000**, *298*, 97.

[14] Boyle, P. D. Growing Crystals That Will Make Your Crystallographer Happy. http://www.xray.ncsu.edu/GrowXtal.html (accessed July 24, 2012).

[15] Sheldrick, G. M. *SADABS and TWINABS—Program for Area Detector Absorption Corrections,* University of Göttingen, Göttingen, Germany, 2010.

[16] Barbour, L. J. *J. Supramol. Chem.,* **2001**, *1*, 189.

[17] Sheldrick, G.M. *Acta Crystallogr., Sect. A: Fundam. Crystallogr.*, **2008**, *64*, 112.